Available online at www.sciencedirect.com
SCIENCE DIRECT®
Nuclear Instruments and Methods in Physics Research A 547 (2005) 583–591
NUCLEAR INSTRUMENTS & METHODS IN PHYSICS RESEARCH Section A
www.elsevier.com/locate/nima

The crossed geometry of two super mirror polarisers—a new method for neutron beam polarisation and polarisation analysis

M. Kreuz, V. Nesvizhevsky, A. Petoukhov, T. Soldner*

Institut Laue Langevin, BP 156, F-38042 Grenoble Cedex 9, France

Received 4 January 2005; received in revised form 16 March 2005; accepted 16 March 2005
Available online 17 May 2005

Abstract

We propose a new arrangement of super mirror polarisers to polarise a white cold or thermal neutron beam. With this method, the dependence of the neutron polarisation on angle and wavelength is suppressed efficiently. For such a neutron beam, the average polarisation can be measured with a precision of better than 10^{-3} using opaque spin filters. Average polarisation values of 0.997 for a cold neutron beam can be obtained. Furthermore, the method can be used for efficient polarisation analysis. Here, however, the precision is limited to a few times 10^{-3} by depolarisation effects. We present the method and results of experimental tests.

PACS: 28.20.−v; 29.90.+r

Keywords: Neutron polarisation; Polarisation analysis; Neutron decay; Spin rotation

1. Motivation

Particle physics experiments with cold polarised neutrons determine parameters of the Standard Model of particle physics (e.g. the quark mixing matrix element V_{ud} [1]) or search for physics beyond the Standard Model (e.g. right handed contribution to weak interaction [2,3], time reversal violation beyond the Standard Model in the transmission of neutrons through matter [4]). Decay experiments with polarised neutrons measure correlations of the type $dW \propto (1 + \xi \boldsymbol{P}\boldsymbol{p})$ between the neutron polarisation $\boldsymbol{P}$ and the momentum $\boldsymbol{p}$ of a decay particle [5]. The error of the polarisation measurement enters directly into the systematic error of the correlation coefficient ξ. Present projects for absolute measurements aim for a relative precision of 10^{-3} and require an adequate precision in the knowledge of polarisation. Previous experiments were often limited by the precision of the polarisation measurement

*Corresponding author.
E-mail address: soldner@ill.fr (T. Soldner).

0168-9002/$ - see front matter © 2005 Elsevier B.V. All rights reserved.
doi:10.1016/j.nima.2005.03.154

[1,3]. Another type of experiments aims to discover small asymmetries in neutron decay or neutron capture reactions. These experiments are not limited by the polarisation value but require the highest possible neutron flux. Finally, in spin rotation experiments, the transmitted polarisation is compared for two different targets or target positions. These experiments require a very homogeneous initial polarisation, whereas the absolute value is less important (see [6] for a discussion of systematic errors).

To summarise, one can distinguish three types of experiments with respect to their requirements for polarisation: (i) experiments requiring the highest polarisation and their knowledge with 10^{-3} precision, (ii) experiments requiring the highest possible neutron flux but a moderate polarisation, and (iii) experiments requiring a very small angular and wavelength dependence of the polarisation. The experiments (i) and (iii) require a high intensity, but it is justified to sacrifice some statistics in order to reduce systematic effects related to polarisation.

For polarising a broad non-monochromatic cold or thermal neutron beam, two techniques are presently available: polarised ^{3}He with its strong spin dependence of the absorption cross-section for neutrons, used as spin filter [7], and super mirror (SM) benders [8] (see Fig. 1(a)). With a polarised ^{3}He spin filter, a spatially homogeneous polarisation can be obtained, but high absolute values are very expensive in terms of neutron intensity. Moreover, the polarisation is strongly wavelength dependent and changes in time because of the relaxation of the ^{3}He polarisation. SM benders are stable in time and show a high transmission and an average polarisation of about 0.98, but with a variation of $\sim 10^{-2}$ in space and of $\sim 10^{-1}$ in wavelength (see Fig. 7). Although, with opaque ^{3}He spin filters [9,10], the polarisation $P(\lambda, \boldsymbol{x})$ at a given wavelength and position can be measured with high precision, the precision of the average beam polarisation is limited by the strong dependences $P = P(\lambda, \boldsymbol{x})$ for both, SM benders and ^{3}He spin filters. The requirements of experiments (i) and (iii) cannot be fulfilled with either of these techniques.

We propose a new method using two SM polarisers in crossed geometry that efficiently suppresses wavelength and angular dependence of the beam polarisation and allows for an average beam polarisation of about 0.997, with only moderate losses in intensity (a factor of 2 compared to the intensity behind a single SM polariser). The average polarisation of such a neutron beam can be measured with a precision of better than 10^{-3}.

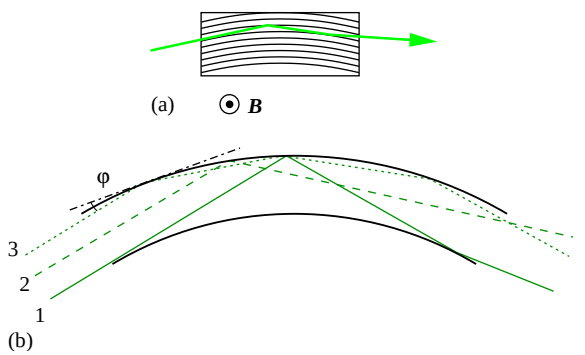

Fig. 1. (a) SM bender (schematic), (b) Sample neutron trajectories in a bender channel.

2. SMs in parallel geometry

In the following, we shortly introduce polarising SM devices. A detailed description of polarising mirrors and SMs can be found in [11].

Neutron polarisation on SMs bases on different reflectivities $R^{\pm}(q_0)$ for the neutrons with spin parallel (+) and antiparallel (−) to the magnetisation vector of a magnetised SM. These reflectivities depend only on the normal component q_0 of the neutron momentum, which is proportional to the ratio φ/λ of the grazing angle $\varphi \ll 1$ and the neutron wavelength λ. The schematic behaviour of $R^{\pm}(\varphi/\lambda)$ is shown in Fig. 2 (see [12,8] for measured examples). The reflectivity is high (1 in case of bulk material where total reflection occurs) for $(\varphi/\lambda) < (\varphi/\lambda)^{\pm}_{\mathrm{crit}}$ and almost 0 for $(\varphi/\lambda) > (\varphi/\lambda)^{\pm}_{\mathrm{crit}}$. Using SM coatings instead of bulk matter aims to increase $(\varphi/\lambda)^{+}_{\mathrm{crit}}$. Nowadays, SMs with $m \equiv (\varphi/\lambda)^{+}_{\mathrm{crit,SM}}/(\varphi/\lambda)_{\mathrm{crit,Ni}} \approx 3$ (relative to unmagnetised natural Ni with $(\varphi/\lambda)_{\mathrm{crit,Ni}} =$

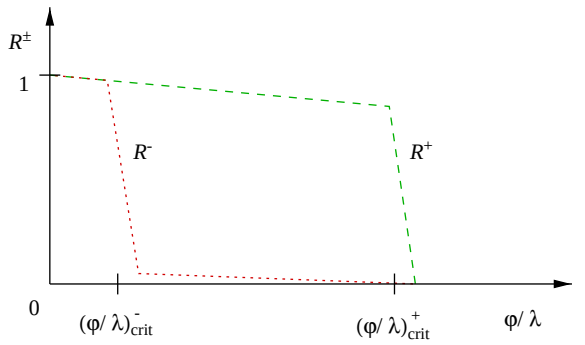

Fig. 2. Reflectivity curves of polarising SMs (schematic).

1.7×10^{-3} rad/Å) are routinely available at the Institut Laue Langevin (ILL).

For a single collision of an unpolarised beam (incoming intensity distribution $I = I(\lambda|x, \varphi)$) on a SM the intensity of reflected neutrons is proportional to the transmission $T^{\pm}$ for the respective spin component:

$$T^{\pm}(\lambda) = \langle R^{\pm}(\varphi/\lambda)\rangle_{I(\lambda|x,\varphi)}. \tag{1}$$

(Here and in the following, we average only over position and angle but not over the wavelength. This corresponds to the usually performed wavelength-resolved measurement.) The resulting polarisation P and transmission T are:

$$P(\lambda) = \frac{T^{+}(\lambda) - T^{-}(\lambda)}{T^{+}(\lambda) + T^{-}(\lambda)}, \tag{2}$$

$$T(\lambda) = T^{+}(\lambda) + T^{-}(\lambda) \approx T^{+}(\lambda). \tag{3}$$

It follows that the properties of a SM polariser depend on the incident beam distribution in wavelength, position, and direction. In particular, the polarisation is limited by $R^{-}(\varphi/\lambda) \to 1$ for $(\varphi/\lambda) \to 0$.

For two subsequent reflections on two SMs with an angle α between them (parallel geometry, Fig. 3(a)), the second collision occurs under the angle $\alpha - \varphi$. The total transmission for the respective spin direction is now

$$\begin{aligned} T^{\pm}_{12}(\lambda) &= \langle R^{\pm}(\varphi/\lambda) R^{\pm}((\alpha-\varphi)/\lambda)\rangle_{I(\lambda|x,\varphi)} \\ &\neq \langle R^{\pm}(\varphi/\lambda)\rangle_{I(\lambda|x,\varphi)} \langle R^{\pm}((\alpha-\varphi)/\lambda)\rangle_{I(\lambda|x,\varphi)}. \end{aligned} \tag{4}$$

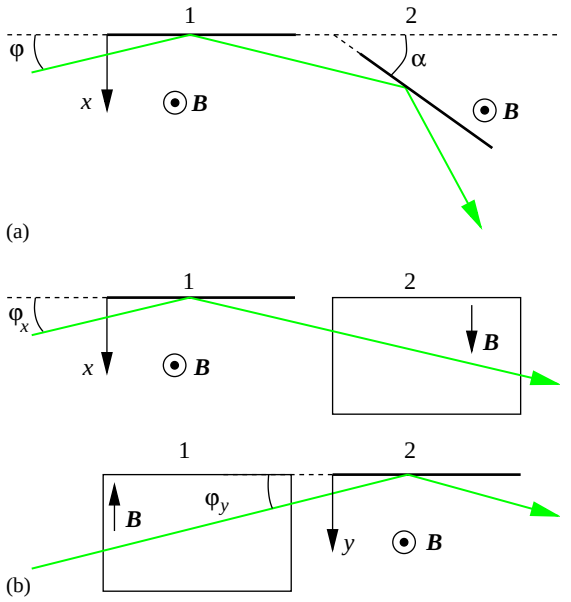

Fig. 3. Reflection of a neutron on two subsequent SM plates: (a) parallel geometry, (b) crossed geometry (projections in y- and x-direction).

Even for this simple geometry, the average transmissions cannot be calculated from the averages for the two SMs. This is also true if the angle does not change between the reflections, i.e. for parallel plates ($\alpha = 0$) and for subsequent reflections on a circularly curved plate ($\alpha = 2\varphi$).

The limitation of the parallel geometry is that two (and more) subsequent devices are always correlated since the neutron trajectory is defined by one and only one independent parameter φ. Beam averaging can therefore not be carried out for the individual devices but only for the full assembly. Consequently, the properties of an assembly of subsequent SM polarisers in parallel geometry (polarising power, transmission) are not intrinsic properties of the polarisers itself but of the assembly at a given incoming (and outgoing) beam. This limits methods of polarisation analysis that assign polarising powers to individual devices and derive the beam polarisation by permuting them or by separating correlated devices (e.g. [13,14]).

3. The crossed geometry

To reduce these limitations of standard geometries of SMs we propose to use two SM devices in crossed geometry (X-SM polarisers, see Fig. 3(b)). This geometry uses an additional degree of freedom in order to polarise the beam, namely the off-plane angle of the parallel geometry Fig. 3(a) (φ_y in Fig. 3(b), see also Fig. 5). Thus, a change of the beam caused by device 1 in its analysed plane does not affect the incident beam with respect to the analysed plane of device 2. The angle averages can be separated now:

$$T^{\pm}_{12}(\lambda) = \langle R^{\pm}(\varphi_x/\lambda)R^{\pm}(\varphi_y/\lambda)\rangle_{I(\lambda|x,\varphi_x,y,\varphi_y)} = T^{\pm}_{1,x}(\lambda)T^{\pm}_{2,y}(\lambda). \quad (5)$$

The polarisation after the combined device can be calculated from the properties of device 1 (with respect to the beam distribution in x-direction) and device 2 (beam distribution in y-direction)

$$P_{12}(\lambda) = \frac{P_{1,x}(\lambda) + P_{2,y}(\lambda)}{1 + P_{1,x}(\lambda)P_{2,y}(\lambda)} \quad (6)$$

$$\approx 1 - \frac{(1 - P_{1,x})(1 - P_{2,y})}{P_{1,x} + P_{2,y}} \approx 1 - \frac{1}{2}(1 - P_{1,x})(1 - P_{2,y}) \quad \text{for } P_{1,2} \approx 1. \quad (7)$$

Eq. (6) is derived in Appendix A. The approximation Eq. (7) shows that an imperfection of the polarising power, $(1 - P)$, is suppressed quadratically in the crossed geometry. Therefore, wavelength and angular dependence of the polarisation should be strongly suppressed. Due to the independence of the devices, a small misalignment of any of the SM plates should change the beam properties negligibly, in contrast to the parallel geometry.

It should be noted that the neutron spin has to be turned adiabatically by $\pi/2$ between the two devices, which can be done by an additional magnetic field (Fig. 4). With the crossed geometry of two SM devices, all degrees of freedom are exploited. For any set-up with more devices, correlations between some of them are unavoidable.

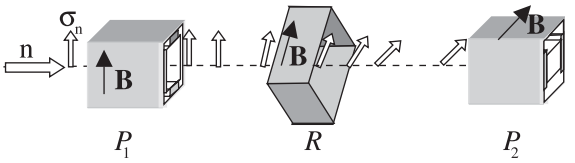

Fig. 4. Set-up of the crossed geometry: two SM polarisers are aligned perpendicular to each other. The neutron spin is transported adiabatically between them.

4. Comparison for SM benders

SM benders which are widely used to polarise a white neutron beam consist of many channels of two curved parallel SMs (see Fig. 1(a), [8]). The channels are long enough to avoid direct view. Sample trajectories are shown in Fig. 1(b). This picture illustrates the significant change of the beam distribution behind the bender with respect to the initial one.

One can distinguish zigzag (reflections on concave and convex side) and garland (reflections only on concave side) trajectories. For a given trajectory, all concave (convex, if there is any) reflections occur at the same grazing angle φ_c (φ_v). For zigzag reflections, since $\varphi_c > \varphi_v$ and because of the shape of the reflectivity curves Fig. 2, the concave grazing angle φ_c is decisive for transmission and polarising power.

The transmission for the spin direction $\pm$ is proportional to $(R^{\pm}(\varphi_c/\lambda))^n$ where n denotes the number of concave collisions for a given trajectory. Neutrons with $|\varphi_c/\lambda| < (\varphi/\lambda)^{\pm}_{crit}$ can be transported for the respective spin direction. The region $|\varphi_c/\lambda| < (\varphi/\lambda)^{-}_{crit}$ remains unpolarised. Since the smallest angles appear for garland reflections, these are the limiting trajectories with respect to the polarising power.

In the limit of an idealised SM coating (i.e. $R^{\pm} = 1$ for $|\varphi_c/\lambda| < (\varphi/\lambda)^{\pm}_{crit}$ and $R^{\pm} = 0$ for $|\varphi_c/\lambda| > (\varphi/\lambda)^{\pm}_{crit}$) only the first collision is decisive and the polarising power does not depend on the number of collisions n. Therefore, a prolongation of the channels beyond the length of direct view is not useful. One can extend this argument and conclude that even for realistic SM coatings (Fig. 2) a second polariser in parallel geometry

being adjusted to maximum transmission is much less efficient than the first one since the same region $|\varphi_c/\lambda| < (\varphi/\lambda)^-_{crit}$ remains unpolarised (see Fig. 5(a)). For a fixed wavelength, the polarisation can be increased by shifting the second polariser from maximum transmission (angle α in Fig. 3(a)), corresponding to a shift between the reflectivity curves of SM 1 and SM 2 in Fig. 5(a). This is not possible for all wavelengths simultaneously. Furthermore, it reduces the angular acceptance of the arrangement and the transmitted intensity. The resulting polarisation depends on the orientation of the two polarisers (angle α) and the neutron wavelength. It cannot be expressed in terms of averaged properties of the individual devices.

For benders in crossed geometry, both devices work with independent angles which increases the polarisation efficiency for all angles including maximum transmission (Fig. 5(b)). Transmission and polarisation efficiency can be calculated from the averaged properties of the first bender with respect to the intensity distribution in x-direction and the second bender with respect to the intensity distribution in y-direction using Eqs. (5) and (6). With typical polarisation values for single SM benders (Fig. 7) a strong suppression of the angular and wavelength dependence and a gain in polarisation is expected for the crossed geometry: the polarisation should be higher than 0.999 up to $\lambda = 6\,\text{Å}$. These properties and the expected moderate loss in intensity make the crossed geometry attractive for beam polarisation and polarisation analysis.

5. Experimental tests and results

The crossed geometry was investigated experimentally at the cold neutron beam facility PF1b [15] of the ILL. The used set-up is shown in Fig. 6. The neutron beam was polarised by two Schärpf SM benders in crossed geometry. It then traversed a resonance flipper, a current sheet flipper, a chopper, and a detector. The neutron spin was guided adiabatically along the flight path. Neutron background was suppressed carefully.

The polarisation was measured by one of the following elements, installed between the chopper and the detector: (a) single SM analyser, (b) X-SM analysers, and (c) polarised ^{3}He spin filters. Cells with different ^{3}He pressures were used in order to cover the full wavelength range. As proposed in Ref. [10], the chosen direction of the ^{3}He polarisation provided low transmission for unflipped neutrons (i.e. polariser and analyser are opposite). This reduces the sensitivity to the flipper inefficiencies. Two flippers were necessary to

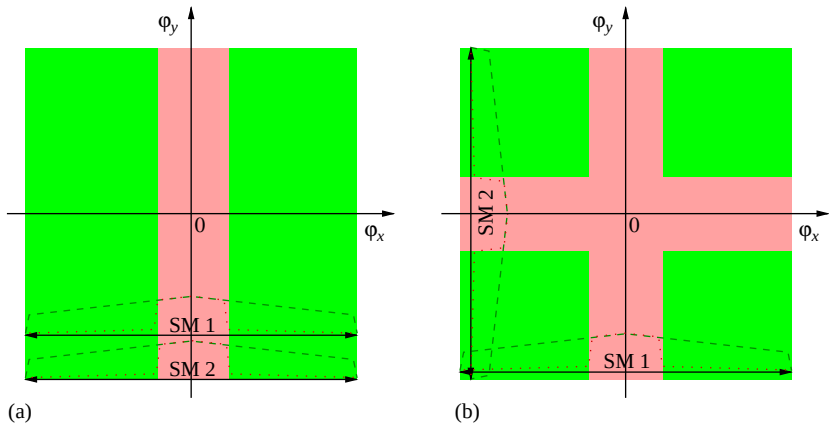

Fig. 5. Comparison of the principles of two parallel (a) and crossed (b) successive SM bender channels. The reflectivity curves R^+ (dashed) and R^- (dotted) are indicated for a fixed wavelength λ. Both devices are adjusted to maximum transmission. For simplicity, the inequivalence of concave ($\varphi > 0$) and convex side ($\varphi < 0$) is neglected (compare text). (a) The two channels use correlated angles resulting in a reduced polarisation efficiency of the second channel. (b) The angles used by the two channels are independent. Both devices enter with their full polarising power.

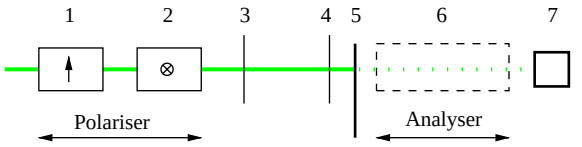

Fig. 6. Set-up for the test measurements: 1–2—X-SM polarisers; 3,4—spin flippers; 5—chopper; 6—different analysers (single SM bender, X-SM analysers, polarised ^{3}He spin filter); 7—detector.

measure the flipping efficiencies for the experiments with SM analysers. The procedures for polarisation analysis with ^{3}He and with two flippers are described in Refs. [10] and [16], respectively.

For the SM analysers, a Schärpf SM polariser ($m = 1.7$) and a modern ILL SM polariser ($m = 2.8$) were used. All SM polarisers and analysers were adjusted to maximum transmission.

Fig. 7(a) compares the wavelength dependences for the measured polarisation products AP (product of beam polarisation and analysing power) for a single SM analyser and for the X-SM analysers.[1] Fig. 7(b) compares the angular dependence of the analysing power for single SM and X-SM analysers. For Fig. 7(b), the analyser (or the assembly of the X-SM analysers) was deflected from maximum transmission.

The absolute value of the polarisation product in the wavelength range between 2 and 6 Å amounted to $AP = 0.992$. Assuming $A = P$, this corresponds to $A = 0.996$ and is below the expected value $A > 0.999$. In order to check for a possible neutron depolarisation in the SM benders, we reduced the magnetic field of the polariser housings serving to magnetise the polarising SM layers. This reduced the polarisation product further. The resulting wavelength dependences are shown in Fig. 8 and compared with the measurement with opaque ^{3}He cells.

The transmission was measured by gold foil activation analysis. The transmission of the used

[1]Note that polarisation and analysing power cannot be separated. For the case of X-SM analysers, $\sqrt{AP}$ can be used to get a rough estimate of the polarisation neglecting correlations and assuming $A \approx P$. A lower limit for P can be fixed assuming $A = 1$.

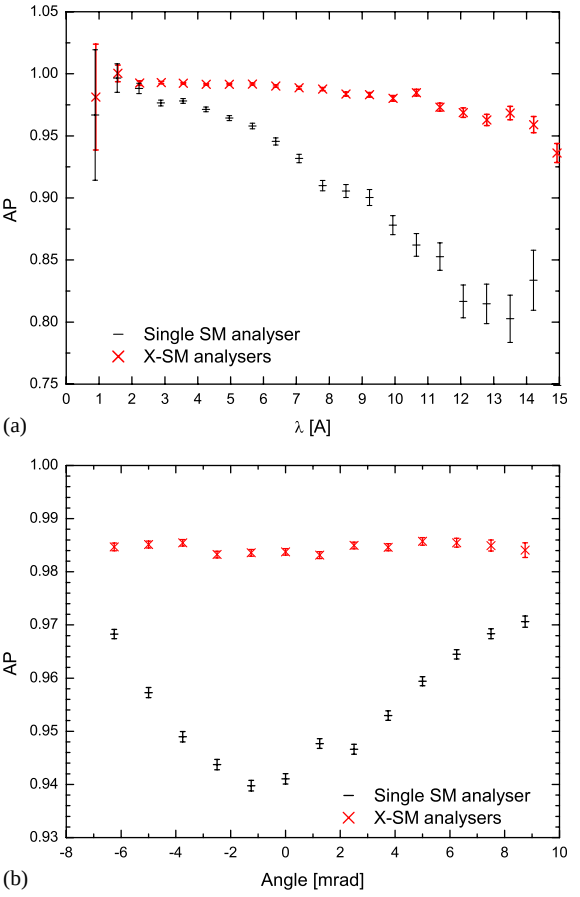

Fig. 7. Measured polarisation products for single SM and X-SM analysers: (a) wavelength dependence, (b) angular dependence (angle 0 mrad corresponds to maximum transmission).

single SM polarisers for the "good" spin component amounts to about 0.5, caused by losses in the support material for the SMs (0.3 mm glass plates, channel width 0.7 mm) and by incomplete transmission inside the channels. With respect to a single SM polariser, the intensity after X-SM polarisers dropped by a factor of 2.

6. Discussion

The expectations for the suppression of wavelength and angular dependence of the polarisation and for the transmission of X-SM polarisers were confirmed experimentally.

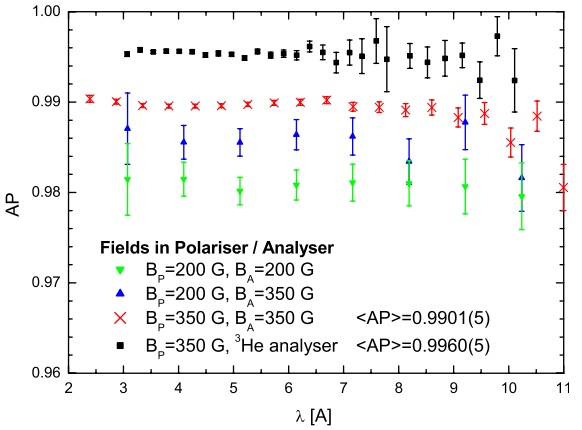

Fig. 8. Polarisation products for different magnetic fields in the polariser housings (X-SM polarisers and analysers) and for opaque polarised ^{3}He as analyser (cells with different ^{3}He pressures were used to cover the presented wavelength range).

On the other hand, the absolute polarisation produced by X-SM polarisers is below the expectation. Since it depends on the magnetic field magnetising the SM and shows no significant dependence on the neutron wavelength, we attribute this to a neutron depolarisation in the reflection on the SM itself. We estimate the depolarisation probability to 0.004 per reflection (only the last reflection is important) for the used Schärpf SM benders with 0.35 kG magnetising field. In general, this value should depend on the specific SM coating but also on the magnetic history of the device (e.g. hysteresis effects).

Zimmer et al. [17] compared spin filters and SM benders for polarisation analysis and found a deviation of 0.001–0.002, which was wavelength independent. The authors give depolarisation in the SM reflection as a possible explanation. In this experiment, other SM analysers with lower critical angle and therefore thicker magnetic layers were used. This could explain the smaller depolarisation probability.

The depolarisation can be reduced by applying a higher magnetic field for the SM magnetisation. The subsequently built PF1b SM polarisers ($m = 2.8$) were equipped with a magnetic field of 1 kG and measurements indicate a depolarisation probability of less than 0.002.

This depolarisation does not limit the application of the method for beam polarisation since the polarisation can be measured precisely using opaque ^{3}He spin filters [9,10]. However, it limits the application for polarisation analysis. In principle, the depolarisation in the analyser can be measured independently and corrected for, but realistic error estimation will imply minimum uncertainties of the order of a few times 10^{-3}. If this precision is sufficient, X-SM analysers are more effective and easier to handle than polarised ^{3}He since they can cover the full wavelength range in one shot. Due to the suppressed angular and wavelength dependence, X-SM analysers are more reliable than SM analysers in other geometries. However, any polarisation analysis with SM analysers is limited by the restricted angular acceptance and by possible correlations between more than two SM devices.

7. Conclusions

For state-of-the-art precision measurements of absolute values of a correlation coefficient between neutron spin and decay particles, X-SM polarisers provide the best means to polarise the neutron beam. The reduction of systematic uncertainties justifies the sacrifice in intensity (0.5 of the intensity after a single bender). High precision polarisation analysis should be performed using opaque spin filters, e.g. polarised ^{3}He, to avoid correlations between different SM devices and uncertainties due to neutron depolarisation. With the new technique, an average polarisation as high as 0.997 can be obtained and measured to a precision of better than 10^{-3}.

For spin rotation experiments, two X-SM polarisers provide a beam of highly polarised neutrons with very high spatial and angular homogeneity (of the order of 10^{-3}). This homogeneity is comparable to what can be achieved with polarised ^{3}He spin filters. Additionally, the beam properties after X-SM polarisers are time and wavelength independent, which is often very important.

X-SM analysers can be used for efficient polarisation analysis, but device-specific depolar-

isation corrections of the order of a few times 10^{-3} and additional uncertainties due to correlations between more than two SM devices and the limited angular acceptance have to be taken into account.

Acknowledgements

We thank our stagaires M. Dehn (Universität Mainz, Germany) and M. Brehm (Universität Heidelberg, Germany) for their enthusiastic help in the experiments. The experiments would not have been possible without the polarised ^{3}He cells provided by H. Humblot, D. Julien, and F. Tasset and without the nice new SM polarisers provided by R. Gähler. Furthermore, we thank M. Thomas for optimising the magnetic housing for the polarised ^{3}He cells and D. Berruyer (all ILL) for preparing many mechanical components of the installation.

Appendix A

A.1. Derivation of Eq. (6)

Applying the transmission for the crossed geometry Eq. (5) to the definition of the polarisation Eq. (2) leads to (the variable λ and the indices x and y are omitted here for simplicity)

$$P_{12} = \frac{T_{12}^{+} - T_{12}^{-}}{T_{12}^{+} + T_{12}^{-}} \tag{A.1}$$

$$= \frac{T_1^{+}T_2^{+} - T_1^{-}T_2^{-}}{T_1^{+}T_2^{+} + T_1^{-}T_2^{-}}. \tag{A.2}$$

Note that this holds only for independent devices.

Eq. (2) and (3) can be rewritten as

$$T^{\pm} = \frac{T}{2}(1 \pm P) \quad (T = T^{+} + T^{-}). \tag{A.3}$$

Applying this for $T_1^{\pm}$ and $T_2^{\pm}$ in Eq. (A.2) results in

$$P_{12} = \frac{(1+P_1)(T_1/2)(1+P_2)(T_2/2) - (1-P_1)(T_1/2)(1-P_2)(T_2/2)}{(1+P_1)(T_1/2)(1+P_2)(T_2/2) + (1-P_1)(T_1/2)(1-P_2)(T_2/2)}$$
$$= \frac{P_1 + P_2}{1 + P_1P_2}. \tag{A.4}$$

Depolarisation is neglected above but could be introduced straightforwardly.

References

[1] H. Abele, M. Astruc Hoffmann, S. Baeßler, D. Dubbers, F. Glück, U. Müller, V. Nesvizhevsky, J. Reich, O. Zimmer, Phys. Rev. Lett. 88 (2002) 211801.
[2] A.-S. Carnoy, J. Deutsch, B.R. Holstein, Phys. Rev. D 38 (1988) 1636.
[3] A.P. Serebrov, I.A. Kuznetsov, I.V. Stepanenko, A.V. Aldushchenkov, M.S. Lasakov, Y.A. Mostovoi, B.G. Erozolimskii, M.S. Dewey, F.E. Wietfeldt, O. Zimmer, H. Börner, JETP 86 (1998) 1074.
[4] V.V. Fedorov, V.V. Voronin, Nucl. Instr. Meth. B 201 (2003) 230.
[5] J.D. Jackson, S.B. Treiman, H.W. Wyld, Phys. Rev. 106 (1957) 517.
[6] S.K. Lamoreaux, R. Golub, Phys. Rev. D 50 (1994) 5632.
[7] K.P. Coulter, A.B. McDonald, W. Happer, T.E. Chupp, M.E. Wagshul, Nucl. Instr. and Meth. A 270 (1988) 90.
[8] O. Schaerpf, Physica B 156–157 (1989) 639.
[9] O. Zimmer, T.M. Müller, P. Hautle, W. Heil, H. Humblot, Phys. Lett. B 455 (1999) 62.
[10] O. Zimmer, Phys. Lett. B 461 (1999) 307.
[11] F. Ott, Etude de couches minces magnétiques par réflectivité de neutrons polarisés. Diffusion hors spéculaire sur des structures périodiques, Ph.D. Thesis, Université Paris XI Orsay, 1998. URL http://www-llb.cea.fr/theses/ott_1998.pdf
[12] O. Schaerpf, Physica B 156–157 (1989) 631.
[13] H. Nastoll, K. Schreckenbach, C. Baglin, A. Bussière, J.P. Guillaud, R. Kossakowski, P. Liaud, Nucl. Instr. and Meth. A 306 (1991) 65.
[14] A.P. Serebrov, A.V. Aldushchenkov, M.S. Lasakov, I.A. Kuznetsov, I.V. Stepanenko, Nucl. Instr. and Meth. A 357 (1995) 503.

[15] H. Häse, A. Knöpfler, K. Fiederer, U. Schmidt, D. Dubbers, W. Kaiser, Nucl. Instr. and Meth. A 485 (2002) 453.
[16] H. Kendrick, S.A. Werner, A. Arrott, Nucl. Instr. and Meth. 68 (1969) 50.
[17] O. Zimmer, P. Hautle, W. Heil, D. Hofmann, H. Humblot, I. Krasnoschekova, M. Lasakov, T.M. Müller, V. Nesvizhevsky, J. Reich, A. Serebrov, Y. Sobolev, A. Vassilev, Nucl. Instr. and Meth. A 440 (2000) 764.